Mediterranean Archaeology and Archaeometry, Vol. 18, No 5, (2018), pp. 109-129

DOI: 10.5281/zenodo.1285889

BUILDING MATERIALS AND ARCHITECTURAL MODELS IN LATE ROMAN TUSCANY. ARCHAEOMETRIC STUDIES ON MORTARS, STONES AND VITREOUS *TESSERAE* FROM "VILLA DELL'ORATORIO" (FLORENCE)

Raneri S.[1,*], Cantini F.[2], Belcari R.[2], Baldanza A.[3], Bertinelli A.[3], Lorenzetti G.[4], Legnaioli S. [4], Mazzoleni P.[5], Lezzerini M. [1,4]

[1]Univeristy of Pisa, Department of Earth Sciences, Via S. Maria 53, 56126 Pisa (Italy)
[2]University of Pisa, Department of Civilization and Forms of Knowledge, Via dei Mille 19, 56126 Pisa (Italy)
[3]University of Perugia, Department of Physic and Geology, Via A. Pascoli, 06123 Perugia (Italy)
[4]Applied and Laser Spectroscopy Laboratory, Institute of Chemistry of Organometallic Compounds, Research Area of National Research Council, Via G. Moruzzi 1, 56124 Pisa (Italy)
[5]University of Catania, Department of Biological, Geological and Environmental Sciences, C.so Italia 57, 95129 Catania (Italy)

Received: 15/10/2017
Accepted: 13/12/2017
**Corresponding author: (simona.raneri@unipi.it)*

ABSTRACT

In the framework of the archeological investigations of an outstanding Roman *Villas* in Tuscany (Villa dell'Oratorio, in the territory of Capraia e Limite, Florence), archaeometric studies have been perfomed with the aim to characterize building and decorative materials and retrace construction phases and manufacture technology. The *Villas*, built in the middle of the 4th century, includes a hexagonal structure, about 30 meters in diameter, decorated with painted wall plasters and beautiful figurative floor mosaics. The structure is equipped with apsed rooms (at least 5), exhibiting similarity with some monumental *triclinia* of Constantinople and Rome. Archaeometric analyses have been carried out on mortars, stones and vitreous *tesserae*, with the aim to identify the raw materials and support the archaeological investigation about cultural models and economic status of the aristocratic owner in the Late Roman Tuscany. Mortars samples from different building units of the *Villas* have been studied through minero-petrographic and thermogravimetric methods. Stone *tesserae* have been analyzed by minero-petrographic and sedimentologic methods, to obtain information on the provenance of the raw materials used. Finally, Raman spectroscopy and SEM-EDS analyses have been performed on vitreous *tesserae*, to obtain information on colouring and opaquening agents. The studies carried out on the building elements suggested that, in spite of iconographic and architectural models proper of the great Mediterranean *villae*, local and spolia raw materials were used in this great construction work.

KEYWORDS: mortars, mosaic, glass tesserae, micro-facies, Arno River, Roman age, Late Roman villa, Vetti's Villa

1. INTRODUCTION

The discovery of great ancient architectural structures, like some Late Roman *Villas*, raises numerous archaeological and historical questions: the property of the building complex, its construction features and phases, architectural models and role in the surrounding area as well in the largest Mediterranean network.

Although the stratigraphic investigation of the buildings and the study of the archaeological artefacts allow us to answer relevant questions, some of them, such as the origin of the raw materials and the technologies used in the construction of the structures, can be investigated only with the support of archaeometric analyses.

For this reason, we applied an interdisciplinary approach to the study of one of these large complexes, namely the Late Roman '*Villa dell'Oratorio*', located in the province of Florence, in the municipality of Capraia and Limite.

The investigations of the '*Villa dell'Oratorio*' took place since 2010, under the direction of the University of Pisa and the Superintendence of Archeological Heritage of Tuscany (until 2015) (Cantini et al., 2017; Lezzerini et al., 2017b) (Figure 1a).

The Late Roman *Villas* was built around the middle of the 4th century on the remains of a former building, probably a villas dated to the Early Imperial Age. It was a great structure that has comparisons in the Mediterranean area in other great Senate and Imperial residences (Baldini Lippolis, 2014; Brogiolo and Chavarrìa Arnau, 2014; Chavarrìa Anrau and Lewit, 2004; Marano, 2016; Turchiano, 2014; Sfameni et al., 2016; Vera, 2012). The building, at least in the second half of the 4th century, probably belonged to the Senator *Vettio Agorio Pretestato* (or a member of his family), who was a prominent figure of the Late Antiquity (Kahlos, 2010), as recalled in a celebratory marble inscription found in the site in 1983 (Figure 1b).

The building reflects the importance of the owner. It includes a hexagonal structure with five apsed rooms (with service environments), which faced a central hexagonal salon, all enriched by mosaic floors (Figure 1c-d). In particular, one room has a central emblem with the representation of a wild boar hunt, while another room has an octagonal pattern filled with geometric and phytomorphic motifs, animals and a human torso. The hexagonal structure can be interpreted as a monumental *triclinium*, finding comparisons in Rome and Costantinople. In Rome, we have the '*Domus* delle Sette Sale', an aristocratic house of the 4th century, with a hexagonal hall on which six rooms are faced (Volpe, 2000), and the so-called 'Minerva Medica Temple', a central plant building, although with twelve sides. Dated at 300 AD, it belonged to the private area of the Constantine *Palatium Sessorium* (Barbera et al., 2014), located about 700 m from the Roman *domus* of Pretestato (Guidobaldi, 1995). In Constantinople, the *Villas* finds comparisons in two hexagonal building dated to the 5th century. One is part of the Palace of the *praepositus sacri cubiculi* Antioco (432-439) (Baldini Lippolis, 2005; Daffara, 2016), in the *regio III*; the other one is a structure dating to the second half of the 5th century, discovered in 1921 in the Gülhane area, and identified with one of the Theodosian properties (Baldini Lippolis, 2005; Daffara 2016).

The hexagonal structure was illuminated by large glass windows, covered by a wooden pyramid dome, probably equipped with a central oculus, and enriched by painted walls and ceilings. In particular, one room probably hosted a *stibadium* in the apse and had its walls decorated with red bands, small black *Kántharos* fountains on a red background and, probably, human figures.

In the west of the hexagonal building there was a thermal complex with circular and hexagonal rooms, found in the recent excavation of the spring 2017.

The complex was expanded during the 5th century: in particular two new rooms, a semicircular tub and a big rectangular building were added. The latter is probably a warehouse. This could suggest that in that period the production management role of the villa was emphasized. This new economic function could be linked to a change in the ownership, which could explain the reuse of the inscription of Pretestato.

It would be extremely suggestive to associate this last phase of the *Villas* with the confiscation of the Senate and Imperial property attributed by Procopius of Caesarea to Teodato, nephew of Teodorico (Procop., Gothic War, I, 2; I, 4). The villa was abandoned in the first half of the 6th century. Recovery of glass, metal and building materials is attested up to the 7th century.

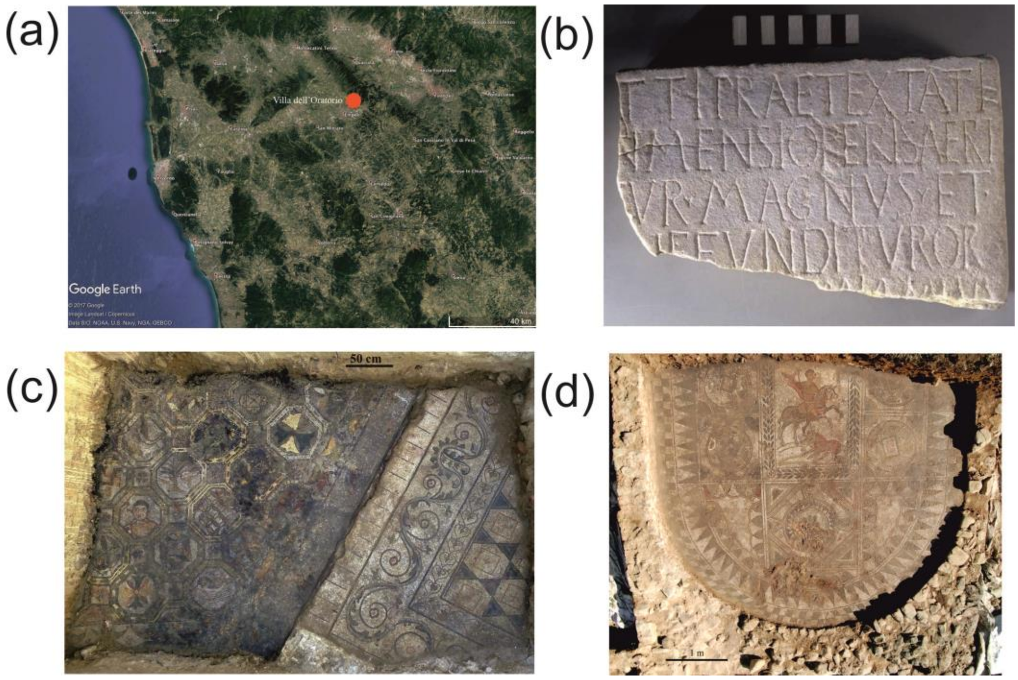

Figure 1. (a) Localization of the site, (b) the marble inscription recalling Senator Vettio Agorio Pretestato, and (c, d) two examples of mosaics.

The archaeological and historical investigation clearly suggest that the architectural paradigms and the decorative patterns of the *Villas* reflect the aristocracy's culture during the 4th century, clearly inspired by supra-regional models. This statement opens several debates about the possible access of clients to building materials imported from Mediterranean areas (a common routine in the early centuries of the Roman Empire) or the potential employment of local raw materials and expertise to resemble the great Late Roman *villas* standards.

The possibility to analyze mosaics, decorative and building stones and glass materials, along with other artifacts and archaeological objects, may allow answering this question, by tracing the raw materials provenance, the artisan routes and possible differences in construction phases.

Multi-disciplinary and multi-methodological approaches are in fact largely applied in archaeological and archaeometric studies with the aim of better understanding and reconstructing the history of complex structures. For example, the characterization of mortars by microscopy (both optical and electronic), thermogravimetric (DSC/DTA/TGA), spectroscopic and micro-chemical methods has been demonstrated as suitable tools for obtaining compositional information (Lezzerini et al., 2014; Pagnotta et al., 2017), identifying construction periods (Antonelli et al. 2012; Miriello et al., 2017; Galello et al., 2017) and determining technological processes and manufacture techniques (Ahmad Bany Yaseen et al., 2013; Cardoso et al., 2014; Drdácký et al., 2013; Riccardi et al., 2007). Moreover, chemical studies of mortars can support conservation studies finalized to produce repair materials (Lopez-Arce et al., 2016; Miriello et al., 2013; Papayianni et al., 2013). As regards to decorative stones, the opportunity to integrate petrographic, mineralogical, chemical, spectroscopic and sedimentological data can allow to discriminate similar rocks (Barone et al., 2013) and determine the provenance of building stones (Baldanza et al., 2012; Brilli et al., 2012; Sammarco et al., 2015; Tasker et al., 2011; Wilkinson et al., 2008), supporting studies about materials circulation, exploitation of quarries and trade. This aspect is particularly relevant in the case of white marbles, traded in antiquity from all the Mediterranean area, for the identification of which petrographic and isotopic analyses are often required (Franzini et al., 2010; Lezzerini et al., 2017a). Recent analytical work on mosaics has been reported in various aims and types (Arinat, 2014; Salama et al., 2017; Kaplan et al., 2017; Nayel and Ali, 2015; Hamarneh, 2015; Sabatino et al., 2016). Finally, the combined chemical and spectroscopic investigation of glass materials can allow to obtain information on technological processes and production models (Arletti et al., 2008; Arletti et al., 2011; Basso et al., 2014; Boschetti et al., 2016; Croveri et al., 2010; Dal Bianco & Russo, 2012; Licenziati & Calligaro, 2016; Moropoulou et al., 2016; van der Werf et al., 2009).

Thus, with the aim to go deeper inside the construction and architectural models employed during the works of '*Villa dell'Oratorio*', mortars (27 samples), stone *tesserae* (598 samples) and glass *tesserae* (100 samples), from the mosaics and the archaeological strata, have been sampled and analyzed by minero-petrographic methods, micro-facies identification, chemical and spectroscopic techniques.

Specifically, the investigation involved:

– the minero-petrographic and compositional analyses of mortars performed by using optical microscopy (OM) and termogravimetric analysis; the obtained data have been compared with already studied mortars sampled from different structures of the *Villas* (Lezzerini et al., 2017b), to highlight possible changes in receipts along the different historical phases identified.

– the isotopic ($^{18}O/^{16}O$ and $^{13}C/^{12}C$ isotopic ratios) and petrographic analyses of white stone *tesserae* sampled from mosaics.

– the petrographic, mineralogical and sedimentological analyses of coloured stone *tesserae* sampled from mosaic, performed by using optical microscopy (OM) and sedimentological study of litho- and micro-facies to identify the provenance of stones and the possible quarries exploited for the manufacture of mosaics.

– the textural and chemical analyses of glass *tesserae*, performed using scanning electron microscopy (SEM-EDS) and Raman spectroscopy, for the characterization and identification of raw materials, colourants and opacifying agents.

2. MATERIALS AND METHODS

2.1. *Studied materials: mortars, stone and glass tesserae*

A total of twenty-seven mortars were sampled from different stratigraphic units (US), accounting structures dated from the end of the 1th century BC to the second half of the 4th century AD, including the *Thermae* and the buildings.

The preliminary macroscopic analysis of materials (colour of the binder, grain size of the aggregate, binder/aggregate ratio, presence and size of the lumps) allowed to identify almost three different groups (Table 1). Group 1 includes samples from the *Thermae* (US 11008, 11009, 11011, 11031, 11055, 11087); they are characterized by binder whitish in colour, presence of lumps up to 1-2 mm, medium cohesion, low binder/aggregate ratio, with aggregates due to medium-coarse sand. Group 2, also accounting samples from the *Thermae* (US 11090 and 11092), are cocciopesto mortars, with low binder/aggregate ratio and high cohesion, mainly employed as wall covering. Finally, Group 3 consists in bedding mortars sampled from the hexagonal structures (US 1614, 1689, 1690, 1691, 12053), and characterized by whitish binder, low cohesion and high binder/aggregate ratio, presence of lumps even 1 cm in diameter, and aggregates mainly due to sub-rounded sandy grains.

Table 1. Sampling and macroscopic features of the mortar samples

Sample ID	US	Dating	Function and structure	Group	Binder colour	Cohesion	Aggregates	Binder/aggregate ratio
M9	11008	Middle-second half of 4th century	bedding mortar, *Thermae*	1	whitish	medium	Medium-coarse sand, sub-rounded grains	low
M 1	11008	Middle-second half of 4th century	bedding mortar, *Thermae*	1	whitish	medium	Medium-coarse sand, sub-rounded grains	low
M 10	11008	Middle-second half of 4th century	bedding mortar, *Thermae*	1	whitish	medium	Medium-coarse sand, sub-rounded grains	low
M 2	11009	End I BC – first quarter of AD	bedding mortar, *Thermae*	1	whitish	medium	Medium-coarse sand, sub-rounded grains	low
M 3	11009	End I BC – first quarter of AD	bedding mortar, *Thermae*	1	whitish	medium	Medium-coarse sand, sub-rounded grains	low
M 4	11009	End I BC – first quarter of AD	bedding mortar, *Thermae*	1	whitish	medium	Medium-coarse sand, sub-rounded grains	low
M 11	11055	End I BC – first quarter of AD	bedding mortar, *Thermae*	1	whitish	medium	Medium-coarse sand, sub-rounded grains	low
M 20	11055	End I BC – first quarter of AD	bedding mortar, *Thermae*	1	whitish	medium	Medium-coarse sand, sub-rounded grains	low
M 5	11011	Middle-second half of 4th century	bedding mortar, *Thermae*	1	whitish	medium	Medium-coarse sand, sub-rounded grains	low
M 27	11011	Middle-	bedding mortar,	1	whitish	medium	Medium-coarse	low

		second half of 4^{th} century	*Thermae*				sand, sub-rounded grains	
M 22	11087	Middle-second half of 4^{th} century	bedding mortar, *Thermae*	1	whitish	medium	Medium-coarse sand, sub-rounded grains	low
M 23	11087	Middle-second half of 4^{th} century	bedding mortar, *Thermae*	1	whitish	medium	Medium-coarse sand, sub-rounded grains	low
M 26	11031	Middle-second half of 4^{th} century	bedding mortar, *Thermae*	1	whitish	medium	Medium-coarse sand, sub-rounded grains	low
M 8	11090	Middle-second half of 4^{th} century	wall covering, *Thermae*	2	reddish-white	high	cocciopesto and fine grained sand	low
M 21	11090	Middle-second half of 4^{th} century	wall covering, *Thermae*	2	reddish-white	high	cocciopesto and fine grained sand	low
M 25	11090	Middle-second half of 4^{th} century	wall covering, *Thermae*	2	reddish-white	high	cocciopesto and fine grained sand	low
M 24	11092	Middle-second half of 4^{th} century	wall covering, *Thermae*	2	reddish-white	high	cocciopesto and fine grained sand	low
M 6	12053	Middle-second half of 4^{th} century	bedding mortar, hexagonal structure	3	whitish	low	fine grained sand; numerous lumps are also present	high
M 7	12053	Middle-second half of 4^{th} century	bedding mortar, hexagonal structure	3	whitish	low	fine grained sand; numerous lumps are also present	high
M 12	1614	Middle-second half of 4^{th} century	bedding mortar, hexagonal structure	3	whitish	low	fine grained sand; numerous lumps are also present	high
M 13	1614	Middle-second half of 4^{th} century	bedding mortar, hexagonal structure	3	whitish	low	fine grained sand; numerous lumps are also present	high
M 14	1614	Middle-second half of 4^{th} century	bedding mortar, hexagonal structure	3	whitish	low	fine grained sand; numerous lumps are also present	high
M 15	1614	Middle-second half of 4^{th} century	bedding mortar, hexagonal structure	3	whitish	low	fine grained sand; numerous lumps are also present	high
M 16	1689	Middle-second half of 4^{th} century	bedding mortar, hexagonal structure	3	whitish	low	fine grained sand; numerous lumps are also present	high
M 19	1690	Middle-second half of 4^{th} century	bedding mortar, hexagonal structure	3	whitish	low	fine grained sand; numerous lumps are also present	high
M 17	1691	Middle-second half of 4^{th} century	bedding mortar, hexagonal structure	3	whitish	low	fine grained sand; numerous lumps are also present	high
M 18	1691	Middle-second half of 4^{th} century	bedding mortar, hexagonal structure	3	whitish	low	fine grained sand; numerous lumps are also present	high

The stone *tesserae* of the mosaics exhibit a wide range of colours, from white to black, gray to red, green to yellow, with various nuances of the same tone (Figure 2a). On the basis of style and figurative units, mosaics can be dated to the middle/second half of the 4^{th} century; iconographic models seem to revoke African repertoires (Cantini et al., 2016), occurring also in other Late Roman *Villae*, such as Villa del Casale in Piazza Armerina (Sicily) (Ariano, 2014). Interesting to note that a slight variation in style can be observed in the central room; this evidence was firstly interpreted in term of a different chronology with respect to the other mosaics, even if recent investigations seem to credibly suggest a change in workers. To go deeper inside aspects related to raw materials and manufactures, *tesserae* representative of the different nuances and almost four room of the Villa (n. 2, 12, 13 and 14, see later

Figure *12*) were sampled directly from mosaics, as well as from the excavated strata on the mosaic floor. Overall, 598 *tesserae* were studied and examined. The average thickness of mosaic elements is 9 ± 1 mm, with a surface area of 153 ± 66 mm^2; white *tesserae* exhibit the highest thickness and surface area (about

10 mm and 121 ± 41 mm^2, respectively), while the thinner *tesserae* are represented by the red and yellow ones.

Glass *tesserae* were recovered from excavated strata and certainly pertained to wall mosaics, not still preserved; they exhibit a wide range of colour (Figure 2b), with a thickness of 4-5 mm and a surface area of about 100 mm^2. Overall, about one hundred glass *tesserae* have been studied; a selection of *tesserae* representative of the different colours and typologies have been thus analyzed by chemical and spectroscopic methods. It is noteworthy that, apart from *tesserae*, the archaeological excavation brought to light also other glass artifacts as well raw glass cakes (in strata dated to 7th century AD), suggesting a glass making activity or, at least, quenching processes.

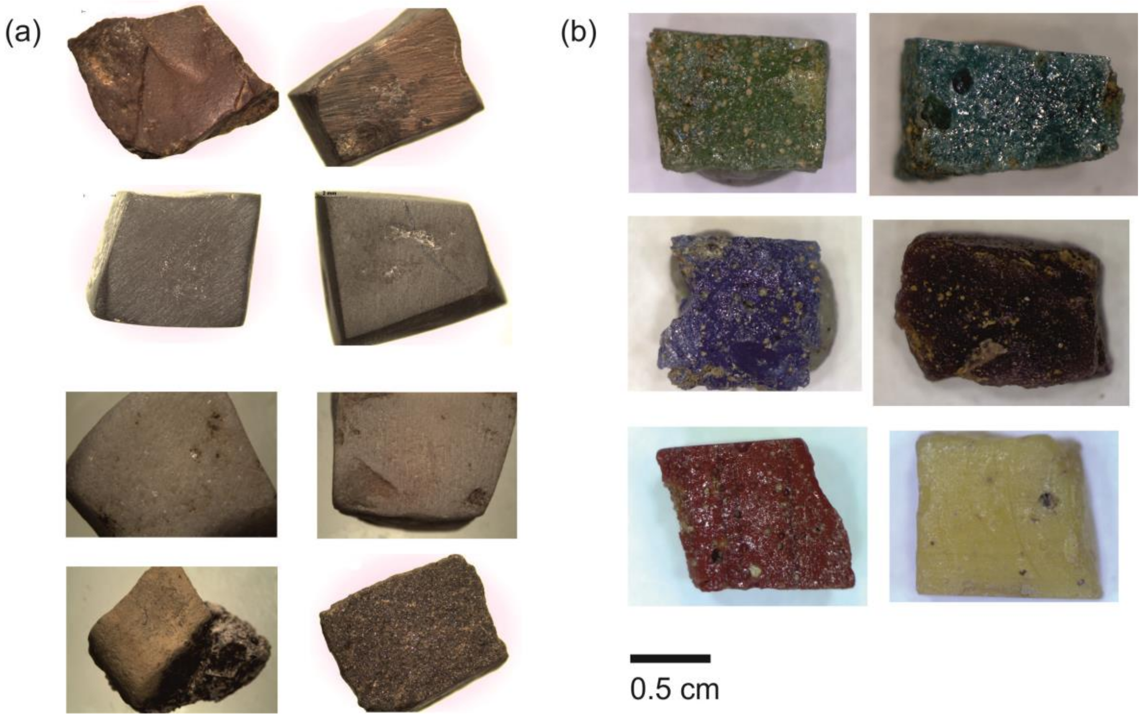

Figure 2. Macroscopic pictures of some representative stone (a) and glass (b) tesserae.

2.2. *Experimental*

Mineralogical and petrographic investigations were carried out on mortars by optical microscopy (OM) on polished thin sections using a Carl Zeiss Axioplan polarizing microscope. Moreover, to classify the hydraulic character of mortars, thermogravimetric analyses (TGA) were obtained on about 25 mg of binder-enriched specimens, dried (silica gel as drying agent) at room temperature for at least a week, using a thermal analyser Netzsch 449 C Jupiter in the following experimental conditions: open alumina crucibles, heating rate of 10°C/min and 30 ml/min nitrogen gas flow.

As regards to stone *tesserae*, a total of 55 pieces, sampled from the mosaics and recovered from the detached materials of the mosaic of Roman '*Villa dell'Oratorio*', were analyzed.

For white marble samples, minero-petrographic features were studied by optical microscope; $^{18}O/^{16}O$ and $^{13}C/^{12}C$ isotopic ratios were measured by mass spectrometry (McCrea, 1950) at the Institute of Geosciences and Earth Resources, National Research Council of Pisa. Carbonate powders were reacted with 100% phosphoric acid at 70°C using a Gasbench II connected to a Thermo Finnigan Five-Plus mass spectrometer. The isotopic ratios of carbon and oxygen were measured in accordance with the international standard Pee Dee Belemnite (PDB) and expressed in delta values $\delta^{13}C$‰ and $\delta^{18}O$‰ (Craig, 1957). The standard error for the delta values is ± 0.1‰ for both carbon and oxygen. The results of mineralogical, petrographic and isotopic analyses were carefully compared with data reported in literature, collecting Mediterranean marbles used in antiquity (Antonelli and Lazzarini, 2015; Capredi and Venturelli, 2004; Franzini and Lezzerini, 2010; Gorgoni et al., 2002; Lazzarini and Antonelli, 2003; Moens et al., 1992).

Coloured stone *tesserae* were studied to characterize the lithological features and to attribute them to peculiar lithofacies, with the aim to individuate the possible source area and the old quarries from which they have been extracted. Fifty *tesserae* were washed and embedded with epoxy resin to prepare thin sections. The obtained thin sections, analyzed under a minero-petrographic microscope, allowed the identification of lithologies and microfacies. Calcareous nannofossil analysis was applied when the stratigraphic attribution was not clearly identifiable by thin section investigation. Smear slides for calcareous nannofossil analysis were prepared following the standard method suggested by Bown (1998), avoiding mechanical or physical processes that could modify the original composition of the assemblage. The slides were analyzed under a Zeiss petrographic microscope at 1000x magnification. Two samples were treated with diluted HF (2%vol) to extract the radiolarian content; unfortunately, the poor preservation of tests does not permit to add further information about the age of siliceous lithologies.

The glass *tesserae* were investigated by applying an integrate approach including SEM-EDS and micro-Raman techniques. In particular, SEM-EDS analysis were performed to investigate the textural and compositional features of both glass matrix and crystalline inclusions. Measurements were performed by a Philips XL30 instrument, equipped with an energy dispersive spectrometry EDAX (standardless software DXi4) with 20 kV acceleration voltage, 0.1 nA beam current, and 100 s live time. On each sample, almost three areas 20 x 20 μm^2 have been analyzed. Additional information about glass structure, opacifier and colourants agents were obtained by Raman spectroscopy analysis; a Renishaw *Raman Invia*, equipped with Leica microscope with 50x objective and CCD detector was used for the analysis. The He:Ne (λ=633 nm) and Nd:YAG (λ=532 nm) laser sources were used for excitation, depending on colour of the *tesserae*.

3. RESULTS

3.1. Mortars

Thin section analysis revealed some textural differences among the studied samples, in accordance with macroscopic observations (Figure 3). Overall, the aggregate is made of from sub-rounded to well-rounded grains of quartz, feldspars and rock fragments, indicating an origin from natural sands. A different aggregate/binder ratio and grain size distribution can be observed for samples of Group 1 and 3; the first group is characterized by a polymodal grain size distribution (from ~0.5 mm to ~1.5 mm in diameter) and low binder/aggregate ratio, while in the second group, aggregates exhibit an unimodal grain size distribution (~0.5-1 mm on average) and an higher binder/aggregate ratio. In mortars of Group 2, aggregates include also cocciopesto fragments, with clear reaction rims. It is noteworthy that mortars belonging to Group 3 exhibit quite similar features with previous studied materials, sampled from both the hexagonal structure and later buildings dated to the 5th century AD (Lezzerini et al., 2017b).

The mineralogical composition of the aggregates, evaluated on the basis of petrographic observations, reveals quite a similar quartz/feldspars ratio (2:1), suggesting a common source for all studied mortars, in spite of the slight texture variability previously pointed out. Apart from aggregate composition, microscopic observations showed the occurrence of both under burnt remains and lumps. Additionally, the intergranular binder and the lumps show an almost similar appearance and consist of micro- to crypto-crystalline carbonate matrix, with amorphous phases typical of hydraulic mortars. Finally, the percentage of void is quite low, mainly due to primary porosity (about 10%) and scarce secondary porosity.

To evaluate the hydraulic character of the mortar binders, and to identify the raw materials used for producing mortars, the mass losses in the temperature range 20–1000°C were measured step-by-step on samples of binder-enriched powders. Data has been plotted on CO_2 vs CO_2/H_2O graph, depicting the theoretical curve for the binders produced through the burning of Alberese marly limestone (grey line), suggested as raw material for mortar and plaster manufacture in previous studies (Lezzerini et al., 2017b). The results of the TGA are in substantial agreement with the expected ones, revealing the employment of the same raw materials over the entire architectural complex (Figure 4). As regards to aggregates, the occurrence of sandy aggregates, which shape and composition indicate a fluvial provenance, suggests the use of Arno sands for mortar manufacture.

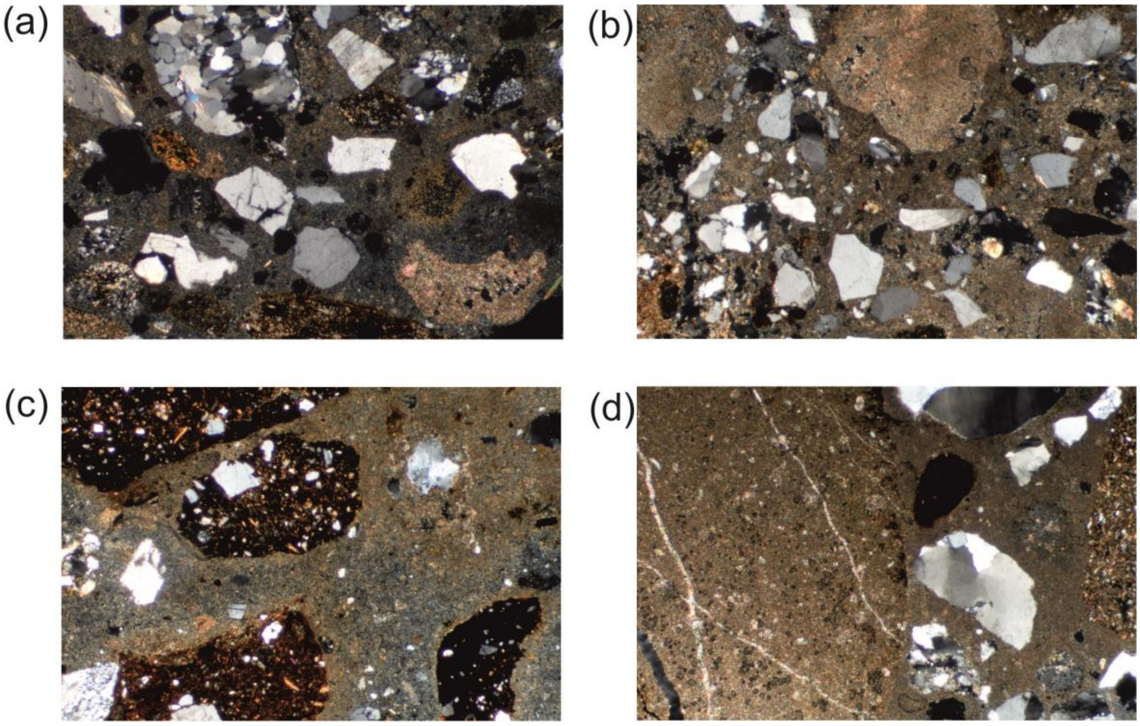

Figure 3. Thin section microphotographs of some selected samples, evidencing (a) mineralogical composition of aggregates, (b) lumps, (c) grog fragments in cocciopesto mortars, and (d) underburned fragments. (The horizontal side of the pictures is 3.3 mm long; crossed polarized light)

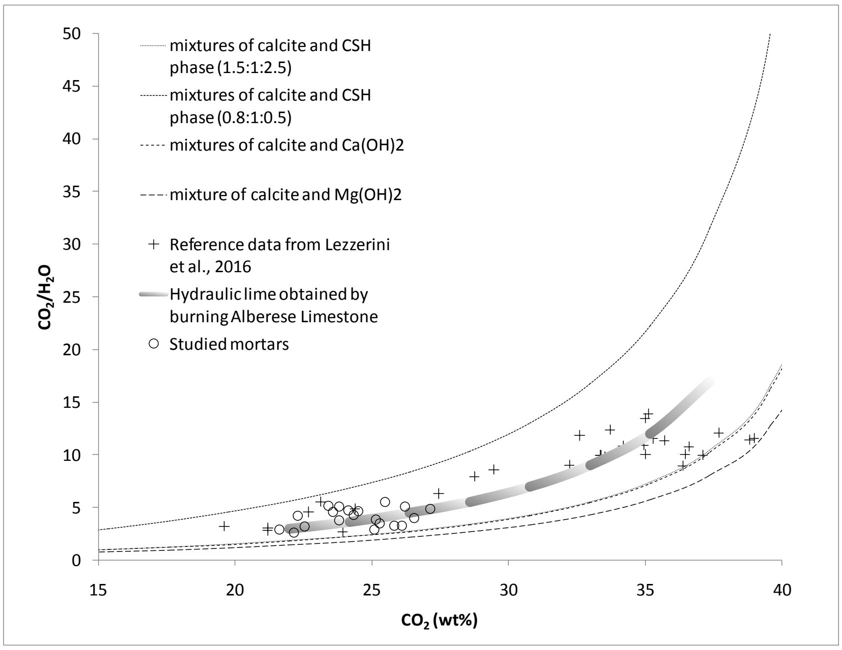

Figure 4. Diagram of CO_2 vs CO_2/H_2O (modified from Lezzerini et al., 2017b)

3.2. *Stone* tesserae

The *tesserae* are very variable in hue; white *tesserae* are mainly due to marbles, while coloured *tesserae* exhibiting similar nuances seem to pertain to different rock types; for this reason, a microfacies investigation was also carried out to define the lithologies.

3.2.1. White *tesserae*: minero-petrographic and isotopic features

White *tesserae* are mainly due to marbles, even if very fine grain limestones and alabastrine litothypes can be also recognized among the sampled stone materials.

As regard marbles *strictu sensu*, white as well as white-gray stone *tesserae* were collected from mosaics and from excavated strata removed from the mosaic floors.

The main petrographic and mineralogical features, along with C-O isotopic ratio, are reported in Table 2, while in Figure 5 thin sections representative of some studied *tesserae* are reported, as example.

Table 2. Minero-petrographic features identified by petrographic observation, C-O isotopic ratios for studied marbles, and possible provenance based on comparison with ancient marble databases. Cal = calcite, Dol = dolomite, Qtz = quartz; Alb = albite; Ho, homeoblastic; He, heteroblastic; G, granoblastic; I, isotropic; M = microgranular; A, anisotropic; w-, weakly-); MGS = Maximum Grain Size.

Sample	Cal	Dol	Other minerals	Texture	MGS (mm)	$\delta^{18}O$ (‰)	$\delta^{13}C$ (‰)	Provenance
WT-1	Only		Alb	Ho, G, I	0.5	-2.12	2.35	Carrara (Italy)
WT-2	Main	Rare		M	0.1	-2.26	1.01	Mt. Pisano (Italy)
WT-3	Main	Rare	Qtz, Mu	w-He, G, w-A	1.2	-4.96	3.24	Mt. Pentelicus (Greece)
WT-4	Main	Sub	Qtz, Ph	He, G (mortar), I	1.9	-2.29	2.15	Prokonnesos (Turkey)

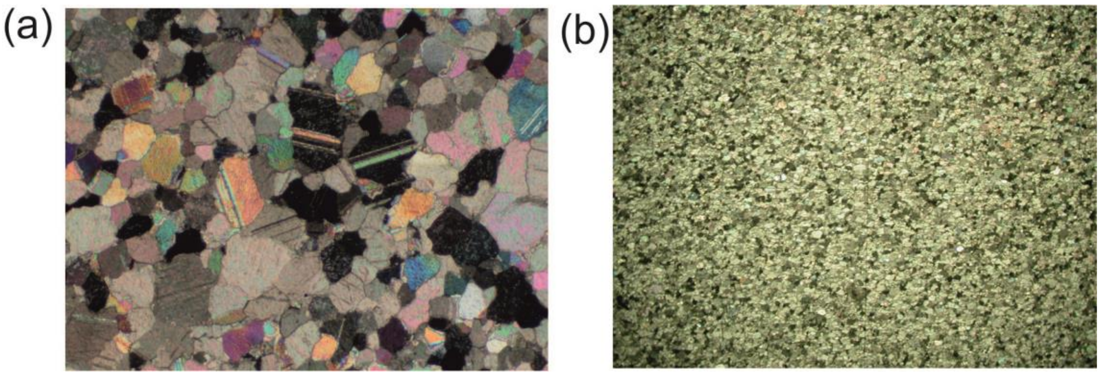

Figure 5. Thin sections of (a) WT1 and (b) WT2, showing the ranging in textural and structural features exhibited by the studied marbles, as example (The horizontal side of the pictures is 3.3 mm long; crossed polarized light)

According to reference data for ancient white marbles (Antonelli and Lazzarini, 2015; Capredi and Venturelli, 2004; Franzini and Lezzerini, 2003; Gorgoni et al., 2002; Moens et al., 1992), the measured maximum grain size (MGS) values range from 0.1 to 1.9 mm and the other petrographic features suggest the occurrence of both local and Mediterranean marbles. By plotting the isotopic data into reference isotopic fields (Antonelli and Lazzarini, 2015; Lezzerini et al., 2012; Franzini and Lezzerini, 2010; Gorgoni et al., 2002; Lazzarini and Antonelli, 2003), a match with local marbles Mt. Pisano, Carrara (Italy), Pentelic (Grecee) and Proconnesian (Turkey) marbles can be observed (Figure 6).

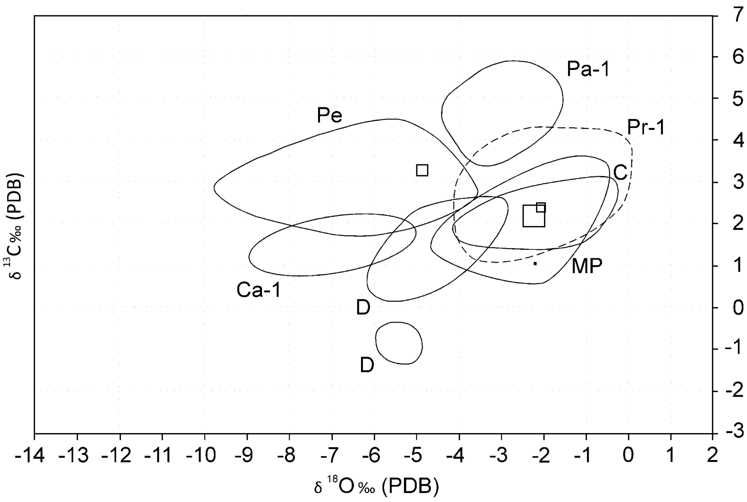

Figure 6. $\delta^{18}O$ vs. $\delta^{13}C$ diagram for Mediterranean marbles used in antiquity and for the studied marble tesserae (empty squares, with dimension according to MGS). Reference isotopic fields from Gorgoni et al., 2002, with supplementary data after Antonelli and Lazzarini, 2015, Lazzarini and Antonelli, 2003, and Franzini and Lezzerini, 2010: C, Carrara; MP, Mt. Pisano; Pe, Mt. Pentelicus; Pr, Prokonnesos, Marmara (Pr-1, main marble).

3.2.2. Coloured *tesserae*: microfacies identification

The thin section analysis allowed the identification of litho-microfacies of almost six different sedimentary rock typologies. All the identified microfacies characters have been compared with literature data (Fazzuoli and Maestrelli-Manetti, 1973; Marcucci et al., 1994; Puccinelli et al., 2009) about the geological units/formations outcropping in the neighboring area of '*Villa dell'Oratorio*' and of other Mesozoic and Cenozoic outcrops.

As reported in Figure 7 and Table 3, the main lithologies used by mosaicists can be classified as carbonatic (56%) and siliceous (12%) rocks, with a minor contribution of a mixed carbonatic/siliceous lithotype (14%) and probable rocks of chemical origin (alabaster, 16%).

All the lithologies are attributable to the Tuscany Succession Units and in particular, from oldest to youngest, to: Calcare selcifero di Limano (LIM), Calcari e Marne a Posidonia (POD), Diaspri (DSD), Maiolica (MAI), Scaglia Toscana (STO) and Macigno (MAC). The acronyms are from the Italian Geological Survey (Geological map 262, Pistoia).

Table 3. Characteristic of litho-micro-biofacies and colour, identified in 50 representative tesserae, attribution to the Geological Formations or biostratigraphic Units, and occurrence (in %) of studied tesserae for each identified litothype.

Lithofacies	Colour	Microfacies	Number of *tesserae*	Fm or Unit attribution	%
Carbonatic limestone	red; pink; light gray-light brown	Wackestone with planktonic and benthic foraminifera and bivalve shell fragments-Cretaceous and Late Paleocene	13	Scaglia Toscana Formation (STO)	26%
Alabaster	cream white and orange-pink		8	(?) Grotta Giusti alabaster	16%
Carbonatic limestone	dark green-light brown; light grey-orange; light pink.	Wackestone with common bioclasts, benthic foraminifera, radiolaria, sponge spicules and ostracods - Early/Middle Jurassic	7	Calcare Selcifero di Limano (LIM)	14%
Biocalcarenite with Qtz and fillo-silicates	dark brown-green	Packstone with bioclasts, macroforaminifera, benthic foraminifera, algae, Qtz crystals and micas. Lower Miocene	7	Macigno (MAC)	14%
Carbonatic limestone	dark red; red	Mudstone with microbioclasts, no microfossils; calcareous nannofossil assemblages of Middle Jurassic	7	Calcari e Marne a Posidonia (POD)	14%
Siliceous wackestone	dark red	Radiolarite with well preserved radiolarians - Middle/Late Jurassic	6	Diaspri Formation (DSD)	12%
Carbonatic limestone	gray-green	Mudstone with rare calcitized radiolaria	2	Maiolica (MAI)	4%

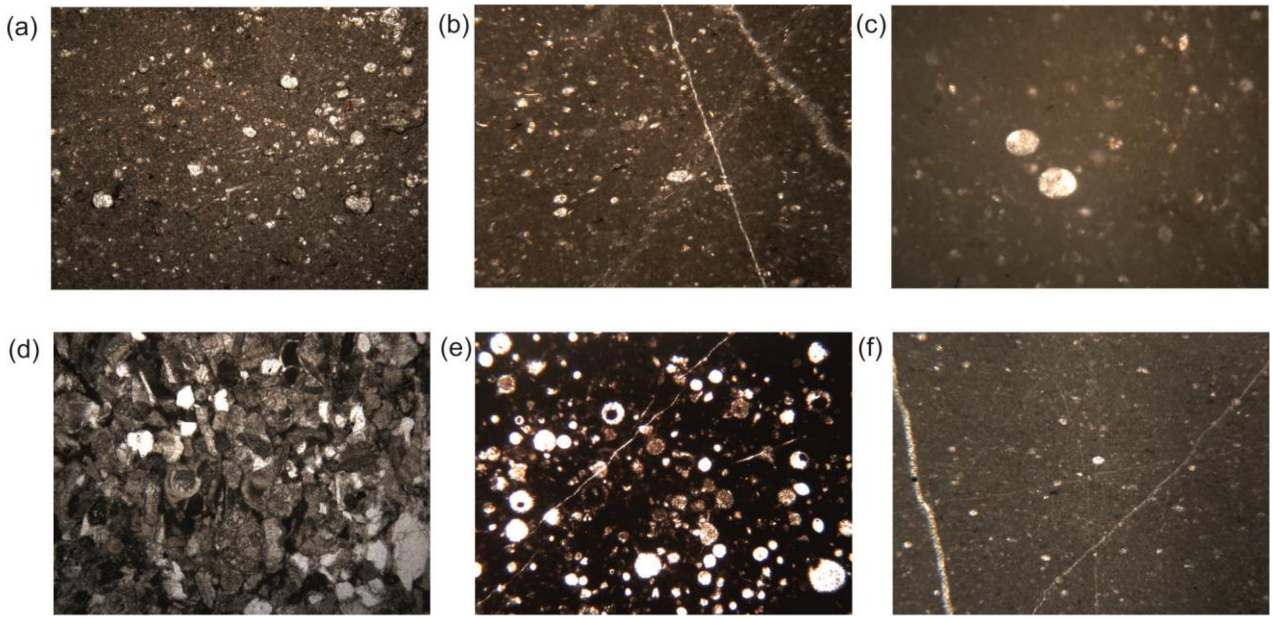

Figure 7. Microphotos of tesserae thin sections. (a) Wackestone with planktonic and benthic foraminifera, sponge spicules and rare bivalve fragments. Cretaceous to Late Paleocene, Scaglia Toscana Fm (STO), x 40; (b) Wackestone with benthic foraminifera, radiolaria, sponge spicules and ostracods. Early-Middle Jurassic, Calcare Selcifero di Limano (LIM), x 2.5.; (c) Mudstone with microbioclasts and rare bivalve shell fragments. Middle Jurassic, Calcari e Marne a Posidonia (POD), x 40; (d) Packstone with macroforaminifera, benthic foraminifera, calcareous algae, common quartz, feldspar and micas crystals. Lower Miocene, Macigno (MAC), x 2.5; (e) Dark red siliceous wackestone with well-preserved radiolarian assemblages of Middle-Late Jurassic. Diaspri Fm (DSD), x 10; (f) Mudstone with rare calcitized radiolaria. Lower Cretaceous, Maiolica Fm (MAI), x 2.5.

These Units crop out in the Monsummano area, located at around 18 km northeast of Limite sull'Arno village, where the Roman '*Villa dell'Oratorio*' is located.

The geology of the Monsummano area is characterized by the anticline of Monte Albano, with NW-SE axis direction and vergence to NE, recumbent in its southern flank. Here, all the units of Tuscany Succession outcrop. Tectonics deeply affected the Monte Albano structure (Puccinelli et al., 2009) originating steep cliffs exploited for lithoid materials, from medieval times until the late 90's.

A short description of the main formations, according to Puccinelli et al. (2009), is following reported, from oldest to youngest:

- Calcare Selcifero di Limano (LIM) - Early Jurassic: Grey or light grey, sometimes graded or often silicified thin to medium bedded limestones and fine calcarenites, with light grey cherty levels and nodules. The more common microfacies are mudstone and wackestone with pellets and bioclasts (radiolarian, benthic foraminifera, sponge spicules, calcareous algae, small bivalves). In Montecatini and Monsummano area, the LIM outcrops with a thickness of 100 m.
- Calcari e Marne a Posidonia (POD) – Middle Jurassic: Grey to green-grey marls and calcareous marls, interbedded with limestone and fine calcarenites (silicified) with rare cherty levels and radiolarites; siliceous clayey levels and grey-green to vine red radiolarites (Marne diasprine) on the top of the unit occur. The microfacies are mudstone and wackestone with bioclasts (radiolarian and thin bivalve shells). The thickness of POD in the Monsummano area is variable from 30 to 50 m.
- Diaspri (DSD) - Middle to Late Jurassic: Diaspri Unit consists of thin bedded red, green to grey cherts and radiolarites. Interbedded claystone and silicified marls became frequent in the upper portion of the unit. In the upper part is present also a discontinuous breccia deposit, yielding siliceous clasts. The radiolarian assemblages indicate for the base of DSD an age from the Upper Bajocian/Lower Bathonian and upper-middle Oxfordian and for the top Upper Tithonian-Lower Berriasian.
- Maiolica (MAI) - Late Jurassic to Early Cretaceous: Maiolica Unit is made of white to grey, limestones, sometimes silicified, with interbedded dark grey calcarenites. Rare grey, grey to green or red thin bedded calcareous or silty argillites are present in the upper part of the unit. The presence of light grey or light brown cherty nodules and lists characterizes the MAI. The microfacies of limestones are represented by mudstone and wackestone with bi-

oclasts (radiolarian and rare calpionellids), the calcarenites are packstone and grainstone with pellets, oolites and bioclasts (radiolarian, benthic foraminifera, fragments of algae and echinoids). Upper Tithonian-Lower Aptian.

- Scaglia Toscana (STO) - Early Cretaceous to Late Oligocene: This unit is constituted by red winy, sometimes greenish grey marls and claystones. The marly portion is more compact than the argillitic one, which is mainly red in colour. This unit mainly outcrops in the western and eastern to south-eastern part of the Monsummano area and it never reaches 100 meters in thickness. The microfacies of mudstones and claystones are wackestone and packstone with planktonic foraminifera. The siliceous facies of STO (known as "Scisti Policromi"sensu Merla et al., 1967) in Monsummano area are characterized by abundant manganese minerals (Marcucci et al., 1994). Stratigraphic range of STO extends from Lower Aptian to Upper Oligocene.

The stratigraphic transition to the Macigno is lacking due to tectonics.

- Macigno (MAC) – Late Oligocene to Early Miocene: Quartz to feldspars graded sandstones, variable in thickness, are characterized by thin interbedded siltstones and claystones. The fresh sandstones (clast size range from fine-medium to coarse) show light-grey colour, which changes in rust and brown if altered.

3.3. Glass *tesserae*

3.3.1. Textural features and glass classification

As regard major elements (Table 4), the raw glass composition of *tesserae* (both opaque and transparent ones) is quite homogenous: SiO_2 ranges from 70 to 64 wt%, Na_2O from 19 to 14 wt%, CaO from 8 to 5 wt% and Al_2O_3 from 3 to 2 wt%. All samples are also characterized by low potash levels, with K_2O ranging from 0.3 % to 0.8%. The orange *tesserae* exhibit the lowest level in silica and sodium (46 and 9 wt%, respectively), and the highest level in lead (PbO = 17.94 wt%). However, we can assume the use of the same raw glass material, as suggested by the inspection of CaO vs. Al_2O_3 diagram (Figure 8a), often employed to discriminate silica sands (Sayre and Smith, 1961).

On the basis of K_2O vs. MgO diagram (see Figure 8b), samples can be classified as natron-based silica-soda-lime glass, peculiar of Roman and Byzantine production in Mediterranean area (Boschetti et al., 2016). Actually, Raman spectra collected on glass *tesserae* exhibit the typical signature of soda-lime-silica glass matrix (see Figure 8c) (Colomban et al., 2006), characterized by strong Q_3–Q_4 components (Si-O stretching, maximum wavenumber ~1094 cm^{-1}) and medium Q_1 and Q_2 (Si-O bending), with additional shoulder at ~950 cm^{-1}, indicating receipts particularly rich in sodium.

Antimony, lead and tin oxides, widely employed as discolouring and opacifying agents, were only detected in opaque *tesserae*.

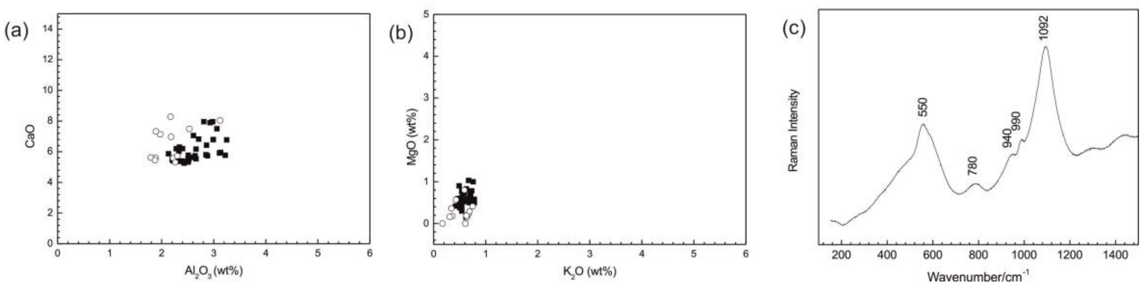

Figure 8. K_2O vs. MgO (a) and CaO vs. Al_2O_3 (b) diagrams for the studied glass tesserae (full square: opaque tesserae; empty circles: transparent tesserae). (c) Raman spectra collected on glass tesserae revealing a natron-based silica-soda-lime composition.

Table 4. SEM-EDS analyses (wt%) of the glass tesserae (on each sample, almost three areas 20 x 20 □m^2 have been analyzed).

Samples	Na_2O	MgO	Al_2O_3	SiO_2	SO	ClO	K_2O	SnO_2	Sb_2O_3	CaO	TiO_2	MnO	FeO	CuO	As_2O_3	PbO	Total
red opaque	18.02	0.55	2.56	64.91	0.25	1.01	0.58	0.21	0.41	5.67	0.09	0.02	1.89	0.88	0.56	2.38	**100**
st.dev.	*0.34*	*0.05*	*0.07*	*1.41*	*0.01*	*0.01*	*0.11*	*0.02*	*0.18*	*0.15*	*0.16*	*0.04*	*0.12*	*0.21*	*0.97*	*2.00*	
yellow opaque	14.61	0.69	3.15	64.17	0.33	0.79	0.61	0.04	0.26	5.88	0.03	0.76	0.48	-	0.80	7.43	**100**
st.dev.	*0.23*	*0.20*	*0.06*	*0.56*	*0.05*	*0.05*	*0.15*	*0.06*	*0.08*	*0.10*	*0.05*	*0.16*	*0.07*	-	*0.69*	*0.96*	
blue opaque	18.17	0.49	2.34	69.22	0.12	1.09	0.52	0.04	0.08	6.24	-	0.80	0.78	-	0.08	-	**100**
st.dev.	*0.20*	*0.12*	*0.06*	*0.27*	*0.00*	*0.03*	*0.02*	*0.07*	*0.08*	*0.06*	-	*0.06*	*0.12*	-	*0.14*	-	
black opaque	16.18	0.68	2.91	66.06	0.13	0.97	0.69	0.09	-	7.94	-	1.01	3.14	0.06	0.00	-	**100**
st.dev.	*0.11*	*0.11*	*0.09*	*0.31*	*0.07*	*0.02*	*0.05*	*0.09*	-	*0.03*	-	*0.10*	*0.38*	*0.10*	*0.00*	-	
orange opaque	9.15	1.01	2.26	46.33	0.56	0.67	0.73	0.69	-	5.98	-	0.08	1.88	9.86	2.62	17.94	**100**
st.dev.	*0.59*	*0.02*	*0.12*	*0.64*	*0.01*	*0.05*	*0.05*	*0.07*	-	*0.09*	-	*0.13*	*0.13*	*0.10*	*0.23*	*0.47*	
violet opaque	16.29	0.55	2.51	67.91	0.06	0.79	0.50	-	1.73	5.50	0.03	3.54	0.43	-	-	-	**100**
st.dev.	*3.78*	*0.03*	*0.13*	*4.07*	*0.00*	*0.04*	*0.01*	-	*0.62*	*0.18*	*0.04*	*0.23*	*0.02*	-	-	-	
aqua opaque	18.54	0.41	2.41	68.70	0.14	1.13	0.51	0.12	0.72	5.43	0.06	0.13	0.44	0.83	-	-	**100**
st.dev.	*0.12*	*0.11*	*0.09*	*1.07*	*0.07*	*0.07*	*0.08*	*0.10*	*0.26*	*0.04*	*0.11*	*0.12*	*0.12*	*0.26*	-	-	
emerald opaque	16.64	0.57	3.01	65.88	0.10	0.89	0.75	0.13	0.21	6.82	0.11	0.78	0.68	3.33	0.11	-	**100**
st.dev.	*0.69*	*0.15*	*0.60*	*0.74*	*0.04*	*0.06*	*0.04*	*0.14*	*0.13*	*0.25*	*0.09*	*0.01*	*0.04*	*0.17*	*0.18*	-	
light green opaque	14.82	0.77	2.83	70.20	0.12	1.01	0.56	0.19	0.50	6.48	0.19	0.10	0.65	1.25	0.36	-	**100**
st.dev.	*5.64*	*0.01*	*0.23*	*3.77*	*0.03*	*0.07*	*0.03*	*0.05*	*0.06*	*0.44*	*0.10*	*0.13*	*0.10*	*0.15*	*0.51*	-	
deep green opaque	17.68	0.31	2.41	69.41	-	0.95	0.57	0.12	0.39	5.32	-	-	0.51	1.43	0.43	-	**100**
st.dev.	*0.10*	*0.15*	*0.11*	*0.95*	-	*0.10*	*0.05*	*0.07*	*0.01*	*0.05*	-	-	*0.12*	*0.30*	*0.42*	-	
blue-green opaque	13.91	0.80	3.16	69.39	0.08	0.92	0.67	0.17	0.10	7.14	0.04	0.83	0.63	1.97	-	-	**100**
st.dev.	*4.08*	*0.04*	*0.13*	*3.04*	*0.11*	*0.11*	*0.05*	*0.01*	*0.14*	*0.52*	*0.05*	*0.02*	*0.18*	*0.50*	-	-	
green-yellow opaque	15.63	0.64	2.92	69.29	0.16	1.03	0.60	0.11	0.55	6.06	0.05	0.06	1.07	0.97	0.37	-	**100**
st.dev.	*4.19*	*0.10*	*0.12*	*3.83*	*0.07*	*0.04*	*0.05*	*0.08*	*0.08*	*0.53*	*0.12*	*0.08*	*0.27*	*0.23*	*0.52*	-	
transparent	17.58	0.39	2.61	67.78	0.16	1.01	0.63	-	-	7.94	0.24	0.93	0.72	-	-	-	**100**
st.dev.	*0.76*	*0.35*	*0.48*	*0.68*	*0.02*	*0.11*	*0.04*	-	-	*0.41*	*0.23*	*0.13*	*0.12*	-	-	-	
transparent	18.82	0.23	2.01	68.12	0.06	0.85	0.68	-	-	7.15	0.05	1.30	0.72	-	-	-	**100**
st.dev.	*0.08*	*0.21*	*0.15*	*0.55*	*0.10*	*0.06*	*0.07*	-	-	*0.18*	*0.08*	*0.22*	*0.18*	-	-	-	
transparent	18.57	0.11	2.12	68.83	0.09	1.24	0.28	-	-	5.50	0.15	1.92	1.18	-	-	-	**100**
st.dev.	*0.34*	*0.10*	*0.21*	*0.13*	*0.03*	*0.12*	*0.10*	-	-	*0.16*	*0.15*	*0.14*	*0.25*	-	-	-	
transparent	18.81	0.37	1.99	68.36	0.06	1.22	0.47	-	-	5.60	0.37	1.76	0.99	-	-	-	**100**
st.dev.	*0,08*	*0,19*	*0,27*	*0,23*	*0,11*	*0,06*	*0,15*	-	-	*0,14*	*0,15*	*0,40*	*0,19*	-	-	-	

Table 5. SEM-EDS analysis (wt%) on particles and grains identified in the opaque tesserae.

Tesserae	Red		Yellow	Black		Emerald					Light green	Deep green	Green-blue						Yellow-green	
Particles	**Cu**	**Cu**	**Sb-Sn-Pb**	**Cu**	**Cu**	**Cu**		**Sb-Sn**		**Cu**	**Sb-Sn**	**Sb-Pb**	**Sb-Sn-Pb**	**Fe**	**Cu**	**Sb-Sn**	**Cu**		**Sb-Sn-Pb**	
wt%																				
Na_2O	-	-	7.78	-	0.64	-	4.3	6.32	8.48	-	8.53	4.47	4.75	0.57	-	9.21	-	3.24	11.65	4.47
MgO	-	-	0.78	-	2.34	-	2.33	0.2	1.01	1.16	1.71	0.45	0.47	0.25	-	5.97	0.39	1.98	0.57	0.45
Al_2O_3	0.17	0.17	10.37	-	1.58	-	2.75	3.51	4.6	0.41	2.58	1.77	3.04	0.4	0.12	5.32	-	2.55	6.46	1.77
SiO_2	0.56	0.56	28.06	0.13	1.2	0.29	11.72	23.1	27.62	1.48	14.38	14.64	17.41	0.43	3.5	4.33	0.18	13.86	38.12	14.64
ZrO_2																				
SO	12.24	12.24	0.76	12.93	-	12.98	0.06	-	0.09	-	0.42	1.57	1.31	0.31	0.03	0.3	-	-	0.82	1.57
ClO	-	-	0.17	-	-	-	0.15	0.1	0.11	-	1.06	0.12	0.16	0.17	0.04	0.32	-	0.16	0.35	0.12
K_2O	-	-	0.54	-	0.44	-	0.63	0.73	0.64	0.17	0.79	0.3	0.2	-	-	0.58	-	0.68	0.54	0.3
SnO_2	-	-	12.79	-	0.99	-	1.71	1.31	1.29	16.98	1.66	1.99	7.55	-	-	2.01	-	1.44	2.38	1.99
Sb_2O_3	-	-	5.77	-	31.04	-	54.22	46.28	40.61	0.45	51.48	17.52	11.88	-	-	53.89	1.99	53.76	7.99	17.52
CaO	-	-	2.85	-	2.55	-	20.99	18.45	12.17	1.53	13.37	3.88	3.16	-	-	16.68	-	21.66	4.53	3.88
TiO_2	-	-	0.28	-	-	-	-	-	-	-	-	1.25	0.97	-	-	0.36	-	-	0.66	1.25
MnO	0.16	0.16	0.16	0.11	0.23	0.05	-	-	0.25	0.15	0.32	-	0	0.21	-	0.37	-	-	0.25	-
FeO	0.32	0.32	1.71	0.49	0.27	0.06	0.22	-	1.2	0.21	0.4	3.02	1.72	97.67	0.08	0.29	0.07	0.47	2.55	3.02
CuO	86.56	86.56	-	86.34	58.73	86.63	0.16	-	0.71	77.45	2.63	-	0.21	-	96.24	0.37	97.37	0.2	0.93	-
As_2O_3	-	-	3.5	-	-	-	0.76	-	-	-	0.66	4.99	1.56	-	-	-	-	-	1.2	4.99
PbO	-	-	24.49	-	-	-	-	-	1.23	-	-	44.03	45.6	-	-	-	-	-	21.02	44.03
Total	**100**	**100**	**100**	**100**	**100**	**100**	**100**	**100**	**100**	**100**	**100**	**100**	**100**	**100**	**100**	**100**	**100**	**100**	**100**	**100**

3.3.2. Colorants and opacifiers

SEM observations carried out on red glass *tesserae* suggest a quite homogenous texture; samples are characterized by Cu-rich crystals, dispersed in the glass matrix, responsible for both colour and opacity (Table 5, Figure 9a). The nature of the Cu-rich particles was inspected by micro-Raman spectroscopy, revealing the presence of cuprite (Cu_2O) as colourant and opacifier agent (Figure 9b). In fact, a strong peak at 218 cm^{-1}, and some weak peaks at 410, 630 cm^{-1} can be ascribed to the characteristic vibrational mode of cuprite (Basso et al., 2014). The peak at 143 cm^{-1} is attributable to stretching vibration of Pb–O, probably related to the opacifying agents. Finally, the occurrence of Fe and Pb in the glass matrix could be interpreted as intentionally added to the melt to prevent copper oxidation and enhance the aspect of the *tesserae*, respectively (Neri et al., 2016).

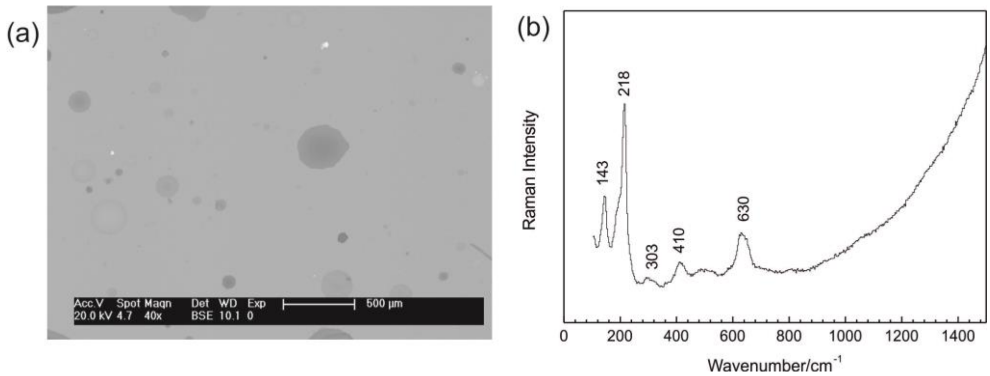

Figure 9. SEM images showing texture and copper particles (a) and Raman spectra (b) representative of red glass tesserae.

As regard yellow *tesserae*, they exhibit quite homogeneous textural features (Figure 10); particles characterised by Sb-Sn-Pb composition are dispersed in the glass matrix (Table 5). This suggests the use of lead-antimoniate, employed as both opacifying and colouring agent, in crystalline phase bindheimite ($Pb_2Sb_2O_7$), as suggested by the inspection of Raman spectra collected on yellow *tesserae* (Figure 10). In fact, three wide peaks at about 331, 452 and 509 cm^{-1} (stretching vibrations of Sb–O and Pb–O bonds) and a very strong peak at about 140 cm^{-1} (stretching vibration of Pb–O) can be associated to lead antimonate in binary Pb–Sb oxide (Basso et al., 2014).

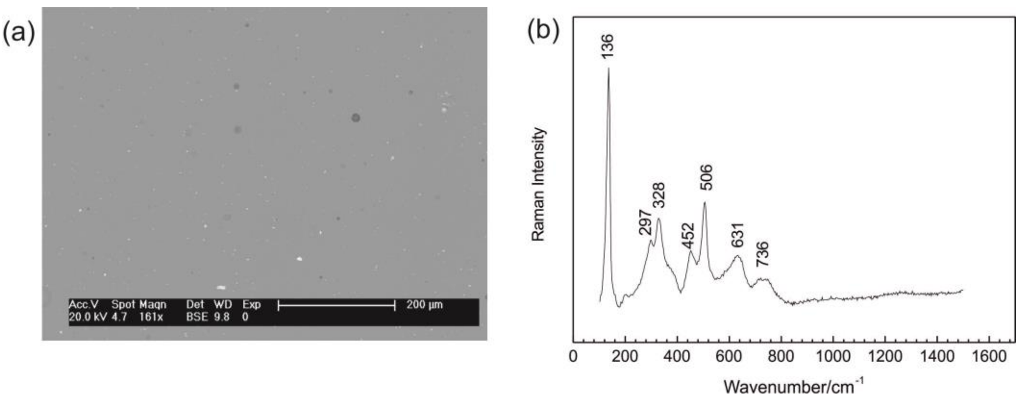

Figure 10. SEM images showing texture and Pb-Sb-Sn opacifiers (a) and Raman spectra (b) representative of yellow glass tesserae.

It is noteworthy that the analyzed particles contain also impurities of iron (1.7 wt% on average) and tin (12.8 wt% on average). The occurrence of Fe and Sn bearing lead-antimony phases is attested for Roman mosaics and has to be related to raw sands containing Pb, Sb, and Sn employed in the preparation of the yellow pigment (Di Bella et al., 2014).

When observed at SEM, light green and yellowish-green *tesserae* show quite homogeneous composition and textural features, with Pb-Sb-rich grains, containing also Sn impurities; moreover, copper-rich grains were detected (Table 5). The occurrence of lead-antimoniate and copper crystals are ascribable to both opacifying and colouring glass matrix: in fact, the combined effect of yellow pyroantimonate and copper give the green nuance to the *tesserae*.

Finally, blue *tesserae*, exhibiting colour ranging from aqua to blue and from emerald to dark blue-green, revealed the presence of high copper contents as crystals dispersed in the glass matrix; additionally, Sb-Ca crystals were also detected, suggesting the use of Ca-antimoniate as opacifier (Table 5, Figure 11). The morphological features of Ca-antimoniate and the Raman spectra collected on samples (peaks at 236, 490 and 667 cm^{-1}, see Figure 11), suggest the use of orthorhombic $Ca_2Sb_2O_7$, used as opacifier in Roman glass (Gedzevičiūtė et al., 2009) and indicating an *in situ* addition procedure for the manufacture of the glass (Di Bella et al., 2014).

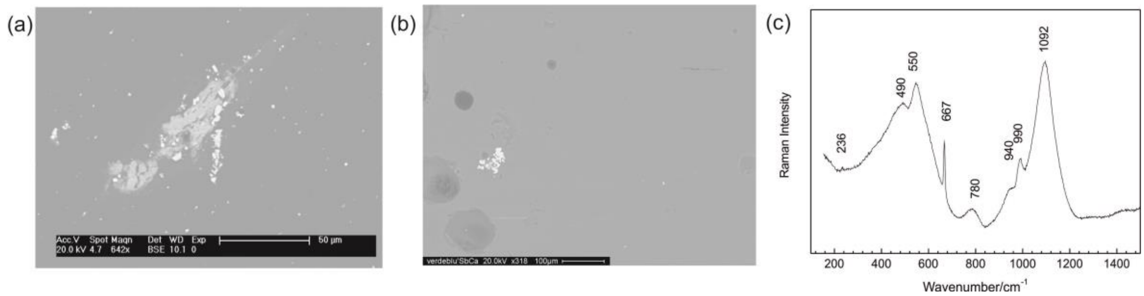

Figure 11. SEM images showing texture and orthorhombic Ca-antimoniate particles (a, b) and Raman spectra (c) collected on aqua tesserae, as representative of blue nuances tesserae.

4. DISCUSSION AND CONCLUSIONS

Archeological and archaometric studies performed on the construction materials of the *Villas* allowed finally to start delineating a complete overview about the possible dynamics developed during the construction works of this interesting structure.

First of all, we noticed that local raw materials were mainly employed for both buildings and mosaics apparatus; however, the occurrence of white marble *tesserae* from Greece and Turkey suggests the reuse of building materials, probably provided as *spolia*. This tendency, which could appear in contrast with the magnificence of the architectural structures of the *Villas*, reflects the contraction of the economy of the Late Roman Period, during which marble slabs were taken from older buildings and stocked to be re-used (Pensabene, 2013).

The artisans responded to this contraction by using *spolia* marbles and adapting the local raw materials to the needs of the aristocracy. They probably experienced the Roman constructive models and traditions in the neighboring cities (Lucca, Pisa and Florence), transposing technological solutions and competences in the rural context. In this regard, they demonstrated to be aware about the raw materials characteristics and related manufacturing solutions, by customizing receipts and processes to different demands. The latter is the case, for example, of mortars; they were made over the time (and specifically for structures which dating spans from 1^h BC to 5^h AD) by using a local marly limestone combined with aggregates from the Arno River. The different mixtures and receipts regards only the function of the structures, without any correlation with the construction phases of the '*Villa dell'Oratorio*' (Figure 12).

The ability of craftsmen involved in the *Villas* construction works to diversify and adopt new solutions in the slip-stream of the Roman tradition is also testified by the accurate selection of stone materials for the manufacture of the mosaic *tesserae*. Locally available through the entire succession of Falda Toscana Unit, they were able to take advantage from the occurrence of different lithotypes characterized by a wide range of colours and tones. The Calcare selcifero di Limano (LIM), Calcari e Marne a Posidonia (POD), Diaspri (DSD), Maiolica (MAI), Scaglia Toscana (STO) and Macigno (MAC) were employed in the impressive mosaics of the hexagonal structure, suggesting the exploitation of the nearby Monsummano-Montecatini outcrops; based on micro-facies studies, it was possible to suggest the Montalbano anticlyne as the source area of these lithotypes. Here, geological formations offer a very large chromatic variability, as well as a quite easy workability, due to the intensive tectonic activity and the availability of stone fragments easily convertible in mosaic *tesserae*.

A Roman tradition could be also recognized in the glass manufacturing routine; raw glass used to produce the studied *tesserae* is compositionally homogeneous and belongs to the so-called natron-based silica–soda–lime glass type. SEM-EDS and micro-Raman investigations on the opaque *tesserae* allowed the identification of colourant opacifier phases, such as metallic copper in the red *tesserae*, lead pyroantimonate in the yellow and green *tesserae* and calcium antimonate phases in the opaque aqua, blue, and emerald *tesserae*. It has to be noticed that a quite relevant similarity can be highlighted with glass *tesserae* employed in the already cited Villa del Casale in Piazza Armerina (Di Bella et al., 2014), with which '*Villa dell'Oratorio*' shares iconographic models, supporting also in this case the idea of a Mediterranean inspiration of the artisans working at the '*Villa dell'Oratorio*'.

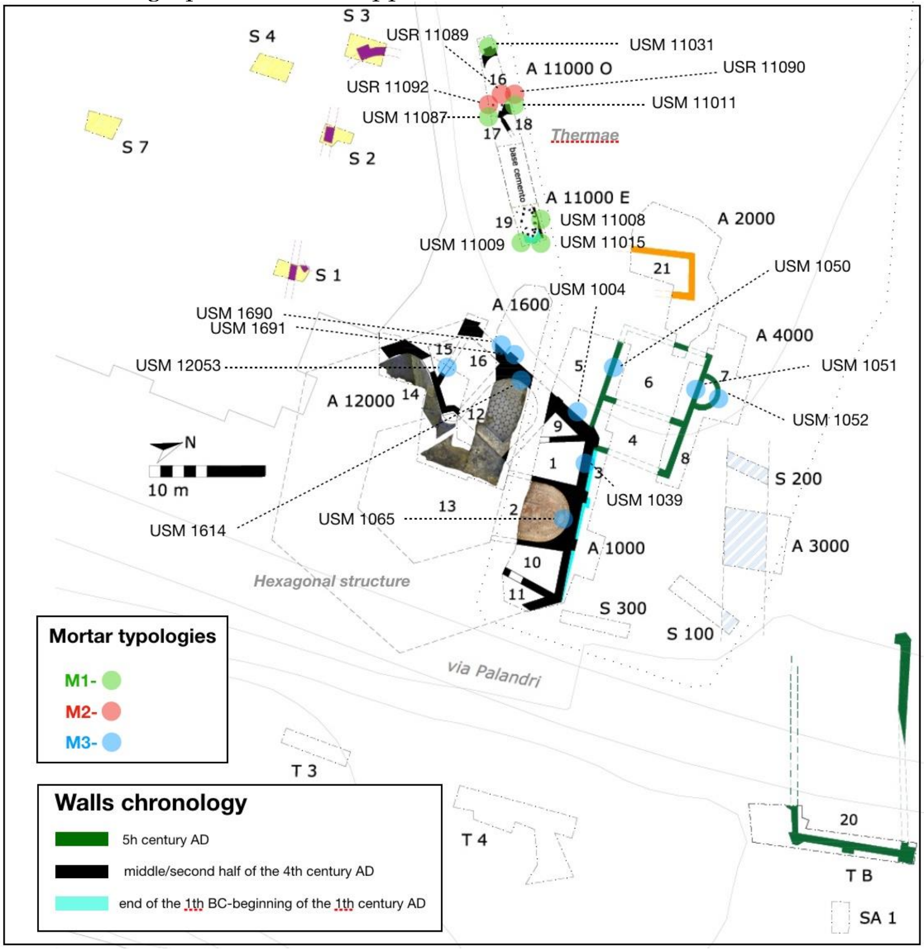

Figure 12. Planimetry of the Villa dell'Oratorio, accounting the different structures along with USM/USR (stratigraphic units) and related mortar groups.

In conclusion, all the obtained results on the studied materials from '*Villa dell'Oratorio*' testify as in the Late Roman Arno Valley craftsmen responded to the demands of the Senate aristocracies by building structures that still reflected Mediterranean architectural models, mostly applying from sophisticated and diversified technology to local or *spolia* materials.

ACKNOWLEDGEMENTS

This work was supported by PRA 2017 (PRA_2017_40, University Research Project) "*Lo spazio del pubblico e del privato dall'antichità al Medioevo: negoziazione di un confine*" bestowed by the University of Pisa (Italy).

REFERENCES

Ahmad Bany Yaseen, I., Al-Amoush, H., Al-Farajat, M., Mayyas A. (2013) Petrography and mineralogy of Roman mortars from buildings of the ancient city of Jerash, Jordan. *Constr. Build. Mater.*, Vol. 38, pp. 465-471

Antonelli F., Lazzarini, L. (2015) An updated petrographic and isotopic reference database for white marbles used in antiquity. *Rendiconti Lincei*, Vol. 26, pp. 399–413.

Antonelli, F., Lazzarini, L., Cancelliere, S. (2012) Minero-petrographic characterisation of the mortars and its possible application in the definition of the building phases. In The fortification of the citadel C. History of warfare, C. Tonghini (ed.), pp. 315–323.

Ariano, C. (2014) I mosaici geometrici di Piazza Armerina: gli influssi degli schemi italici. In *La villa restaurata e i nuovi studi sull'edilizia residenziale tardoantica, Atti del Convegno Interuniversitario di Studi* *sull'edilizia abitativa tardoantica nel Mediterraneo (CISEM)*, P. Pensabene, C. Sfameni (eds.), Bari, pp. 69-77.

Arinat, M (2014) In situ mosaic conservation: a case study from Khirbet Yajuz, Jordan. *Mediterranean Archaeology and Archaeometry,* Vol. 14, No 2, pp. 67-76

Arletti, R., Conte, S., Vandini, M., Fiori, C., Bracci, S., Bacci, M., & Porcinai, S. (2011) Florence baptistery: chemical and mineralogical investigation of glass mosaic tesserae. *Journal of Archaeological Science*, Vol. 38, pp. 79–88.

Arletti, R., Quartieri, S., Vezzalini, G., Sabatino, G., Triscari, M., & Mastelloni, M. A. (2008) Archaeometrical analyses of glass cakes and vitreous mosaic tesserae from Messina (Sicily, Italy). *Journal of Non-Crystalline Solids*, Vol. 354, pp. 4962–4969.

Baldanza, A., Gioncada, A., Lezzerini, M. (2012) Historical building stones of the western Tuscany (Italy): the Acquabona Limestones from Mts. Livornesi. *Periodico di Mineralogia*, Vol. 81, pp. 1-17.

Baldini Lippolis, I. (2005) *L'architettura residenziale nelle città tardoantiche*, Roma.

Baldini Lippolis, I. (2014) Palatia, praetoria ed episcopia: alcune osservazioni. In *La villa restaurata e i nuovi studi sull'edilizia residenziale tardoantica, Atti del Convegno Interuniversitario di Studi sull'edilizia abitativa tardoantica nel Mediterraneo (CISEM)*, P. Pensabene, C. Sfameni (eds.), Bari, pp. 163-170.

Barbera, M., Magnani Cianetti, M., Barrano, S. (2014) Da Massenzio a Costantino: le indagini nel c.d. tempio di Minerva Medica. In *La villa restaurata e i nuovi studi sull'edilizia residenziale tardoantica, Atti del Convegno Interuniversitario di Studi sull'edilizia abitativa tardoantica nel Mediterraneo (CISEM)*, P. Pensabene, C. Sfameni (eds.), Bari, pp. 255-266.

Barone, G., Crupi, V., Longo, F., Majolino, D., Mazzoleni, P., Raneri, S., Venuti, V. (2013) A multi-technique approach for the characterization of decorative stones and non-destructive method for the discrimination of similar rocks, *X-Ray Spectrometry*, Vol. 43, pp. 83-91.

Basso, E., Invernizzi, C., Malagodi, M., La Russa, M. F., Bersani, D., Lottici, P. P. (2014) Characterization of colorants and opacifiers in roman glass mosaic tesserae through spectroscopic and spectrometric techniques. *Journal of Raman Spectroscopy*, Vol. 45, pp. 238–245.

Boschetti, C., Henderson, J., Evans, J., Leonelli, C. (2016) Mosaic tesserae from Italy and the production of Mediterranean coloured glass (4rd century BCE–4th century CE). Part I: Chemical composition and technology. *Journal of Archaeological Science: Reports*, Vol. 7, pp. 303–311.

Bown, P.R. (1998) Calcareous Nannofossil Biostratigraphy. Kluwer Academic Publishers, Dordrecht, pp. 314.

Brilli, M., Antonelli, F., Giustini, F., Lazzarini, L., Pensabene, P. (2010) Black limestones used in antiquity: the petrographic, isotopic and EPR database for provenance determination. *J. Archaeol. Sci.*, Vol. 37, pp. 994–1005.

Brogiolo, G.P. and Chavarría Arnau, A. (2014) Villae, praetoria e aedes publicae tardoantichi in Italia settentrionale: riflessioni a partire da alcune ricerche recenti. In *La villa restaurata e i nuovi studi sull'edilizia residenziale tardoantica, Atti del Convegno Interuniversitario di Studi sull'edilizia abitativa tardoantica nel Mediterraneo (CISEM)*, P. Pensabene, C. Sfameni (eds.), Bari, pp. 227-239.

Cantini, F., 2017 (ed.), La villa dei "Vetti" (Capraia e Limite, Fi): archeologia di una grande residenza aristocratica nel Valdarno tardoantico, Archeologia Medievale, XLIV, pp. 9-71.

Cantini, F., Ramacciotti, M., Alderighi, L., Lezzerini, M. (2016) La villa dell'Oratorio a Capraia e Limite (Fi). Primi dati sulla decorazione parietale. In *Pitture murali nell'Etruria romana: testimonianze inedite e stato dell'arte*, F. Donati (ed.), Pisa, pp. 117-127.

Capedri, S., Venturelli, G., Photiades, A. (2004) Accessory minerals and δ18O and δ13C of marbles from the Mediterranean area. *Journal of Cultural Heritage*, Vol. 5, pp. 27-47.

Cardoso, I., Macedo, M.F., Vermeulen, F., Corsi, C., Santos, S. A., Rosado, L., Candeias, A., Mirao J. (2014) A multidisciplinary approach to the study of archaeological mortars from the town of Ammaia in the roman province of Lusitania (Portugal). *Archaeometry*, Vol. 56, pp. 1-24

Chavarría Arnau, A. and Lewit, T. (2004) Archaeological Research on the Late Antique Countryside. A Bibliographical Essay. In *Late Antique Archaeology. 2. Recent Research on The Late Roman Countryside*, Bowden W., Lavan L., Machado C. (eds.), Leiden-Boston, pp. 3-51.

Colomban, P., Tournie, A., Bellot-Gurlet, L. (2006) Raman Identification of glassy silicates used in ceramic, glass and jewellry: a tentative differ- entiation guide. *Journal Raman Spectroscopy*, Vol. 37, pp. 841-852.

Columbu, S., Antonelli, F., Lezzerini, M., Miriello, D., Adembri, B., Blanco, A. (2014) Provenance of marbles used in the Heliocaminus Baths of Hadrian's Villa (Tivoli, Italy), *Journal of Archaeological Science*, Vol. 49, pp. 332-342.

Craig, H. (1957) Isotopic standards for carbon and oxygen and correction factors for mass-spectrometric analysis of carbon dioxide. *Geochemical and Cosmochemical Acta*, Vol. 12, pp. 133-149.

Croveri, P., Fragalà, I., & Ciliberto, E. (2010) Analysis of glass tesserae from the mosaics of the "Villa del Casale" near Piazza Armerina (Enna, Italy). Chemical composition, state of preservation and production technology. *Applied Physics A*, Vol. 100, pp. 927–935.

Daffara D. (2016), *L'edificio di Gülhane a Costantinopoli: nuove osservazioni*. Thiasos, 5, pp. 69-88.

Dal Bianco, B., Russo, U. (2012) Basilica of San Marco (Venice, Italy/Byzantine period): Nondestructive investigation on the glass Mosaic Tesserae. *Journal of Non-Crystalline Solids*, Vol. 358, pp. 368–378.

Di Bella, M., Quartieri, S., Sabatino, G., Santalucia, F., Triscari, M. (2014) The glass mosaics tesserae of "Villa del Casale" (Piazza Armerina, Italy): a multi-technique archaeometric study. *Archaeological and Anthropological Sciences*, Vol. 6, pp. 345–362.

Drdácký, M., Fratini, F., Frankeová, D., Slížková Z. (2013) The roman mortars used in the construction of the Ponte di Augusto (Narni, Italy) – a comprehensive assessment. *Constr. Build. Mater.*, Vol. 38, pp. 1117-1128

Fazzuoli, M., Maestrelli-Manetti, O. (1973) I nuclei Mesozoici di Monsummano, Montecatini Terme e Marliana (Provincia di Pistoia). *Mem. Soc. Geol. It.*, Vol. XII, pp. 39-79.

Franzini M., Lezzerini M. (2003) The stones of medieval buildings in Pisa and Lucca provinces (western Tuscany, Italy). 1 – The Monte Pisano marble. *Eur. J. Mineral.*, Vol. 15, pp. 217-224.

Franzini, M., Lezzerini, M., Origlia, F. (2010) Marbles from the Campiglia Marittima area (Tuscany, Italy). Eur. J. Mineral., Vol. 22, pp. 881-893.

Gallello, G., Ramacciotti, M., Lezzerini, M., Hernandez, E., Calvo, M., Morales, A., Pastor, A., De la Guardia, M. (2017) Indirect chronology method employing Rare Earth Elements to identify Sagunto Castle mortar construction periods. *Microchemical Journal*, Vol. 132, pp. 251-261.

Gedzevičiūtė, V., Welter, N., Schüssler, U., Weiss, C (2009) Chemical composition and colouring agents of Roman mosaic and millefiori glass, studied by electron microprobe analysis and Raman microspectroscopy. *Archaeological and Anthropological Sciences*, Vol. 1, pp. 15-29.

Gorgoni, C., Lazzarini, L., Pallante, P., Turi, B. (2002) An updated and detailed mineropetrographic and C-O stable isotopic reference database for the main Mediterranean marbles used in antiquity. In *Asmosia 5: Interdisciplinary Studies on Ancient Stone*, J.J. Herrmann, N. Herz, R. Newman (eds.), pp. 115-131.

Guidobaldi, F. (1995) Domus: Vettius Agorius Praetextatus. In *Lexicon Topographicum Urbis Romae, II*, E.M. Steinby (ed.), Roma.

Hamarneh, C (2015) Understanding early Islamic mosaic production: archaeometric study of material from Qasr Mushatta. *Mediterranean Archaeology and Archaeometry*, Vol. 15, No 3, pp. 249-258 (DOI: 10.5281/zenodo.32067).

Kahlos M. (2010) Vettio Agorio Pretestato. Una vita senatoriale nella transizione, Forlì.

Kaplan, Z, Ipekoglu, B and Boke, H (2017) Physicochemical properties of glass tesserae in Roman terrace house from ancient Antandros (base glass, opacifiers and colorants). *Mediterranean Archaeology and Archaeometry*, Vol. 17, No 1, pp. 141-157 (DOI: 10.5281/zenodo.258103).

Lazzarini, L., Antonelli, F. (2003) Petrographic and isotopic characterisation of the marble of the island of Tinos (Greece). *Archaeometry*, Vol. 45, pp. 541–552.

Lezzerini, M., Di Battistini, G., Zucchi, D., Miriello, D. (2012) Provenance and compositional analysis of marbles from the medieval Abbey of San Caprasio, Aulla (Tuscany, Italy). *Applied Physic A*, Vol. 108, pp. 475-485.

Lezzerini, M., Legnaioli, S., Lorenzetti, G., Palleschi, V., Tamponi, M. (2014) Characterization of historical mortars from the bell tower of St. Nicholas church (Pisa, Italy). *Construction and Building Materials*, Vol. 69, pp. 203–212.

Lezzerini, M., Antonelli F., Gallello, G., Ramacciotti, M., Parodi, L., Alberti, A., Pagnotta, S., Legnaioli, S., Palleschi, V. (2017a) Provenance of marbles used for building the internal spiral staircase of the bell tower of St. Nicholas Church (Pisa, Italy). *Applied Physics A*, Vol. 123, pp. 385.

Lezzerini, M., Ramacciotti, M., Cantini, F., Fatighenti, B., Antonelli, F., Pecchioni, E., Fratini, F., Cantisani, E., Giamello, M. (2017b) Archaeometric study of natural hydraulic mortars: the case of the Late Roman Villa dell'Oratorio (Florence, Italy). *Archaeological and Anthropological Sciences*, Vol. 9, pp. 603-615.

Licenziati, F., Calligaro, T. (2016) Study of mosaic glass tesserae from Delos, Greece using a combination of portable µ-Raman and X-ray fluorescence spectrometry. *Journal of Archaeological Science: Reports*, Vol. 7, pp. 640–648.

Lopez-Arce, P., Tagnit-Hammou, M., Menendez, B., Mertz, J.D., Guiavarc'h, M., Kaci, A., Aggoun, S., Cousture, A. (2016) Physico-chemical stone-mortar compatibility of commercial stone-repair mortars of historic buildings from Paris. *Construction and Building Materials*, Vol. 124, , pp. 424-441

Marano, Y. (2016) Gli ambienti absidati nell'architettura residenziale dell'Italia settentrionale tardoantica. In L'alimentazione nell'Antichità, Atti della XLVI settimana di studi aquileiesi, G. Cuscito (ed.), Antichità Altoadriatiche, LXXXIV, pp. 111-130.

Marcucci, M., Cabella, R., Passerini P. (1994) Early late Cretaceous radiolarian deposits in Northern Apennines: biostratigraphy and mineralogical data from the «Scisti Policromi» in the Tuscan succession near Monsummano, Tuscany. *Palaeopelagos*, Vol. 4, pp. 23-34.

McCrea, J.M. (1950) On the isotopic chemistry of carbonates and a paleotemperature scale. *Journal of Chemical Physics*, Vol. 18, pp. 849-857.

Merla, G., Bortolotti, V., Passerini, P. (1967). *Carta Geologica d'Italia alla scala 1:100.000*. Note illustrative del Foglio 106 Firenze. Servizio Geologico d'Italia, Roma, pp. 61.

Miriello, D., Lezzerini, M., Chiaravalloti, F., Bloise, A., Apollaro, C., Crisci, G.M. (2013) Replicating the chemical composition of the binder for restoration of historic mortars as an optimization problem. *Computers and Concrete*, Vol. 12, pp. 553-563.

Miriello, D., Barba, L., Blancas, J., Bloise, A., Cappa, M., Cura, M., De Angelis, D., De Luca, R., Pecci, A., Taranto, M., Yavuz, H.B., Crisci, G.M. (2017) New compositional data on ancient mortars from Hagia Sophia (Istanbul, Turkey). *Archaeological and Anthropological Sciences*, Vol. 9, pp. 499-514.

Moens, L., De Paepe, P., Waelkens, M. (1992) Multidisciplinary research and cooperation: keys to a successful provenance determination of whitemarbles used in antique artifacts. In *Ancient stones: quarrying, trade and provenance*, M. Waelkens, N. Herz, L. Moens (eds.), pp. 247-255.

Moropoulou, A., Zacharias, N., Delegou, E.T., Maróti, B., Kasztovszky, Zs. (2016) Analytical and technological examination of glass tesserae from Hagia Sophia. *Microchemical Journal*, Vol. 125, pp. 170-184.

Nayel, S and Ali, M (2015) Analytical investigation of materials used in the construction of Islamic mosaics in Al Sultan el Mansour Kalaoun School, Cairo, Egypt. *Mediterranean Archaeology and Archaeometry*, Vol. 15, No 2, pp. 163-173 (DOI:10.5281/zenodo.16608).

Neri, E., Morvan, C., Colomban, P., Guerra, M. F., Prigent, V. (2016) Late Roman and Byzantine mosaic opaque "glass-ceramics" tesserae (5th-9th century). *Ceramics International*, Vol. 42, pp. 18859–18869.

Pagnotta, S., Lezzerini, M., Ripoll-Seguer, L., Hidalgo, M., Grifoni, E., Legnaioli, S., Lorenzetti, G., Poggialini, F., Palleschi, V. (2017) Micro-Laser-Induced Breakdown Spectroscopy (Micro-LIBS) Study on Ancient Roman Mortars. *Applied Spectroscopy*,Vol. 71, pp. 721-727.

Papayianni, I., Pachta, V., Stefanidou, M. (2013) Analysis of ancient mortars and design of compatible repair mortars: The case study of Odeion of the archaeological site of Dion. *Construction and Building Materials*, Vol. 40, pp. 84-92

Pensabene, P. (2013) *I marmi nella Roma antica*, Carocci (ed.), Roma, pp. 101-111.

Puccinelli, A., D'amato Avanzi, G., Perilli, N., Verani, M. (2009) – Note Illustrative della Carta Geologica d'Italia alla scala 1:50.000, Foglio 262 Pistoia (foglio Pistoia) 262. Servizio Geologico d'Italia, pp. 161.

Riccardi, M.P., Lezzerini ,M., Carò, F., Franzini, M., Messiga, B. (2007) Microtextural and microchemical studies of hydraulic ancient mortars: two analytical approaches to understand pre-industrial technology processes. *Journal of Cultural Heritage*, Vol. 8, pp. 350-360.

Sabatino, G, Di Bella, M, Quartieri, S, Giuliano, A, Italiano, F, Marciano, G Tripodo, A, Romano, D (2016) Verifying the reliability of historical sources through a mineralogical and petrographic approach : The case of the "black-green stone" from the Messina Cathedral (Sicily, Italy). *Mediterranean Archaeology and Archaeometry*. Vol.16, No.3, 2016 pages: 79-91.

Salama, K.K, Ali, M.F, Moussa, A.M (2017) The presence of cement mortars in the added chambers of El Sakakeny Palace: a case study. *SCIENTIFIC CULTURE*, Vol. 3, No 3, pp. 25-29 (DOI: 10.5281/zenodo.813134)

Sammarco, M., Margiotta, S., Foresi, L.M., Ceraudo, G. (2015) Characterization and provenance of building materials from the Roman Pier at San Cataldo (Lecce, Southern Apulia, Italy): a lithostratigraphical and micropaleonthological approach. *Mediterranean Archaeology and Archaeometry*, Vol. 15, pp. 101–112.

Sayre, E.V., Smith, R.W., 1961. Compositional categories of ancient glass. *Science*, Vol. 9, pp. 1824–1826.

Sfameni, C., Luvidi, L., Stella, E.M., Volpi, M. (2016) Nuovi mosaici e nuove ricerche presso la villa romana di Cottanello (RI). In *Atti del XXI Colloquio dell'AISCOM*, C. Angelelli, D. Massara, F. Sposito (ed.), Tivoli, pp. 235-243.

Tasker, A., Wilkinson, I. P., Fulford, M. G., Williams, M. (2011) Provenance of chalk tesserae from Brading Roman Villa, In *Proceedings of the Geologists' Association*, Isle of Wight, UK, pp. 933-937.

Turchiano, M. (2014) Edilizia residenziale e spazi del lavoro e della produzione nelle ville di Puglia e Basilicata tra Tardoantico e Altomedieovo: riflessioni a partire da alcuni casi di studio. In *La villa restaurata e i nuovi studi sull'edilizia residenziale tardoantica, Atti del Convegno Interuniversitario di Studi sull'edilizia abitativa tardoantica nel Mediterraneo (CISEM)*, P. Pensabene, C. Sfameni (eds.), Bari, pp. 367-380.

van der Werf, I., Mangone, A., Giannossa, L. C., Traini, A., Laviano, R., Coralini, A., Sabbatini, L. (2009) Archaeometric investigation of Roman tesserae from Herculaneum (Italy) by the combined use of complementary micro-destructive analytical techniques. *Journal of Archaeological Science*, Vol. 36, pp. 2625-2634.

Vera, D. (2012) Questioni di storia agrarian tardoromana: schiavi, coloni, villae. *Antiquité Tardive*, Vol. 20, pp. 115-122.

Volpe, R. (2000) *La domus delle Sette Sale, in Aurea Roma. Dalla città pagana alla città cristiana*, S. Ensoli, E. La Rocca (eds.), Roma, pp. 159-160.

Wilkinson, I., Williams, P. M, Young, J. R., Cook, S. R., Fulford, M. G., Lott, G. K. (2008) The application of microfossils in assessing the provenance of chalk used in the manufacture of Roman mosaics at Silchester. *Journal of Archaeological Science*, Vol. 35, pp. 2415-2422.